Towards the FE prediction of permanent deformations of offshore wind power plant foundations using a high-cycle accumulation model

T. Wichtmann, A. Niemunis & Th. Triantafyllidis
Institute of Soil Mechanics and Rock Mechanics, Karlsruhe Institute of Technology, Germany

ABSTRACT: The paper discusses a possible application of the authors' high-cycle accumulation (HCA) model for the prediction of long-term deformations of offshore wind power plant (OWPP) foundations. The calibration of the HCA model parameters for a typical North Sea fine sand is presented. These parameters have been used for exemplary finite element calculations of a monopile foundation, with variation of soil density, average load and cyclic load amplitude.

1 INTRODUCTION

Numerous offshore wind parks will be installed in the North Sea and in the Baltic Sea during the next years. The foundations of offshore wind power plants (OWPPs) are subjected to a multiaxial high-cyclic loading due to wind and waves, which may cause an accumulation of permanent deformations. The serviceability of the OWPPs may get lost due to an excessive tilting of the tower. No established methods for a prediction of the long-term deformations exist so far.

Experience from conventional offshore foundations (e.g. oil rigs) cannot be easily adapted since the ratio of the horizontal cyclic load and the own weight of the structure is significantly larger for the new OWPPs. While existing offshore wind parks lay in relatively shallow water, the water depths will be up to 40 m at the locations of the new offshore wind parks. Therefore, the bending moments at the seabed level will be much larger for the new OWPPs. Furthermore, the new OWPPs will have larger dimensions than the existing ones due to increased power generation requirements. For example, monopiles with diameters between 5 and 8 m will be installed. Practical experience with such large pile diameters in combination with high ratios of cyclic horizontal load and self weight of the structure is missing. Existing methods for the prediction of long-term deformations were developed and proven for much smaller pile diameters and for lower cyclic loads. The applicability of these methods to the new OWPPs is questionable (Section 2).

The present paper discusses a possible application of the authors' high-cycle accumulation (HCA) model (Niemunis et al., 2005) for finite element (FE) predictions of the permanent deformations of OWPP foundations.

2 LITERATURE REVIEW

The guidelines for the design of OWPP foundations published by the certifier Germanischer Lloyd (2005) demand an investigation of both, the short-term and the long-term soil-structure interaction under cyclic loading. However, the methods and the extent of such investigations are not further specified. It is stated that neither a theory nor established investigation methods exist with respect to the long-term behaviour. It is recommended to utilize experience from similar projects in the past, which are missing in the case of the new OWPPs. As a possible approach the adherence of given maximum deflections under a static equivalent load is mentioned but judged as possibly non-conservative.

Both, the recommendations of the American Petroleum Institute (1993) and the Offshore Standard DNV-OS-J101 (Det Norske Veritas, 2004) utilize p-y-curves in order to predict lateral deformations of piles subjected to horizontal loads. In the case of cyclic loading p is reduced. Based on tests of Reese et al. (1974), the API standard proposes a constant reduction factor 0.9. Since the load amplitude, the number of cycles and the soil conditions are not considered, such reduction seems to oversimplify the problem according to the authors' opinion. The DNV standard recommends to use "suitable" p-reduction factors, which are not further specified. A calculation of the cumulative deformations in the soil in a "suit-

able manner" is demanded by DNV, but no respective method has been specified or recommended.

Some more sophisticated modifications of p-y-curves considering the influence of a cyclic loading have been proposed in the literature (Welch and Reese, 1972; Swinianski and Sawicki, 1991; Long and Vanneste, 1994; Little and Briaud, 1988). For example, Little and Briaud (1988) proposed to increase y with N according to $y(N) = y(N = 1)\ N^a$, where the parameter a can be obtained from cyclic pressuremeter tests. However, an extrapolation of the pressuremeter data obtained for small numbers of cycles to large N-values seems doubtful.

It should be kept in mind that all these methods and equations recommended in the standard codes or proposed in the literature were developed for smaller pile diameters, lower ratios of cyclic horizontal load and self weight of the structure, and smaller number of cycles. The applicability to the large pile diameters of the new OWPPs in combination with the large cyclic horizontal loading has not been confirmed yet.

This lack of knowledge served as a motivation for ongoing research on the long-term behaviour of the new OWPP foundations. Different approaches are followed. Achmus et al. (2008) calculated the lateral displacements with an elastoplastic constitutive model, reducing the constrained elastic modulus M in dependence of the number of load cycles and the load amplitude. Lesny and Hinz (2006) described a method in which the permanent deformations are predicted using a strain wedge model. The stress-strain behaviour of the soil is derived from a multi-stage cyclic triaxial test. Based on model tests and FE calculations, Dührkop (2010) proposed a p-reduction factor which increases linearly from zero at the seabed level to 0.9 for $z/L > 0.5$ with L being the pile length. Since in-situ measurements are not available yet for the new OWPP foundations, all these methods were calibrated or proven based on small-scale model tests or measurements at smaller pile diameters. Therefore, at present it is unclear if these procedures are able to predict realistic permanent deformations.

The authors of the present paper intend to predict the permanent deformations of OWPP foundations by means of finite element calculations using their high-cycle accumulation model.

3 HIGH CYCLE ACCUMULATION MODEL

The main constitutive equation of the HCA model reads

$$\dot{\boldsymbol{\sigma}} = \mathsf{E} : (\dot{\boldsymbol{\varepsilon}} - \dot{\boldsymbol{\varepsilon}}^{\text{acc}} - \dot{\boldsymbol{\varepsilon}}^{\text{pl}}) \tag{1}$$

with the Jaumann stress rate $\dot{\boldsymbol{\sigma}}$ of the effective Cauchy stress $\boldsymbol{\sigma}$, the strain rate $\dot{\boldsymbol{\varepsilon}}$, the prescribed strain accumulation rate $\dot{\boldsymbol{\varepsilon}}^{\text{acc}}$, the plastic strain rate $\dot{\boldsymbol{\varepsilon}}^{\text{pl}}$ (for stress paths touching the yield surface only) and the pressure-dependent elastic stiffness E. In the high-cyclic context "rate" means the derivative with respect to the number of cycles N. The accumulation rate is calculated as the product of the scalar *intensity* of accumulation $\dot{\varepsilon}^{\text{acc}}$ and of the *direction* of accumulation $\mathbf{m}$ (a unit tensor):

$$\dot{\boldsymbol{\varepsilon}}^{\text{acc}} \;=\; \dot{\varepsilon}^{\text{acc}}\,\mathbf{m} \;=\; f_{\text{ampl}}\; \dot{f}_N\; f_e\; f_p\; f_Y\; f_\pi\; \mathbf{m} \tag{2}$$

The flow rule of the modified Cam clay (MCC) model has been experimentally found to approximate $\mathbf{m}$ well. A multiplicative approach is used for $\dot{\varepsilon}^{\text{acc}}$. Each function considers separately the influence of a different parameter (Table 1, f_{ampl}: strain amplitude, f_e: void ratio, f_p: average mean pressure p^{av} (that means the average value of mean pressure p during a cycle), f_Y: average stress ratio $\eta^{\text{av}} = q^{\text{av}}/p^{\text{av}}$, $\dot{f}_N$: cyclic preloading, f_π: polarization changes). The spatial field of the strain amplitude can be obtained from a calculation of a few cycles using a conventional constitutive model. The authors use hypoplasticity with intergranular strain (von Wolffersdorff, 1996; Niemunis and Herle, 1997) for that purpose.

Table 1. HCA model functions and parameters for the tested fine sand ($e_{\min}$ = 0.677, $e_{\max}$ = 1.054).

Function	Mat. const.	Value
$f_{\text{ampl}} = \left(\varepsilon^{\text{ampl}}/10^{-4}\right)^{C_{\text{ampl}}}$	C_{ampl}	1.31
$f_e = \dfrac{(C_e - e)^2}{1+e}\ \dfrac{1+e_{\max}}{(C_e - e_{\max})^2}$	C_e	0.58
$f_p = \exp\left[-C_p\ (p^{\text{av}}/100 - 1)\right]$	C_p	0.22
$f_Y = \exp\left(C_Y\ \bar{Y}^{\text{av}}\right)$	C_Y	1.85
$\dot{f}_N = \dot{f}_N^A + \dot{f}_N^B$	C_{N1}	$2.82 \cdot 10^{-4}$
$\dot{f}_N^A = C_{N1} C_{N2} \exp\left[-\dfrac{g^A}{C_{N1} f_{\text{ampl}}}\right]$	C_{N2}	0.37
$\dot{f}_N^B = C_{N1} C_{N3}$	C_{N3}	$2.64 \cdot 10^{-5}$

4 CALIBRATION OF THE HCA MODEL FOR A FINE SAND

The HCA model parameters have been determined for a uniform fine sand (d_{50} = 0.14 mm, $C_u = d_{60}/d_{10} = 1.5$). This sand is also currently used in small-scale model tests on OWPP foundations performed at our institute. It is intended to verify the accuracy of the HCA model prediction by recalculations of these model tests.

Stress-controlled drained cyclic triaxial tests with 10^5 load cycles applied at a frequency of 0.2 Hz have been performed in order to determine the parameters C_{ampl}, C_e, C_p, C_Y, C_{N1}, C_{N2} and C_{N3} (Table 1). Four different amplitudes, seven different initial relative densities I_{D0}, four different average mean pressures p^{av} and four different average stress ratios $\eta^{\text{av}} =$

$q^{\text{av}}/p^{\text{av}}$ have been tested in separate tests. No multi-stage tests have been performed. Figure 1 shows a typical plot of the vertical strain $\varepsilon_1(t)$ measured during the first 24 cycles and during five cycles recorded at N = 50, 100, 200, ..., 10^5.

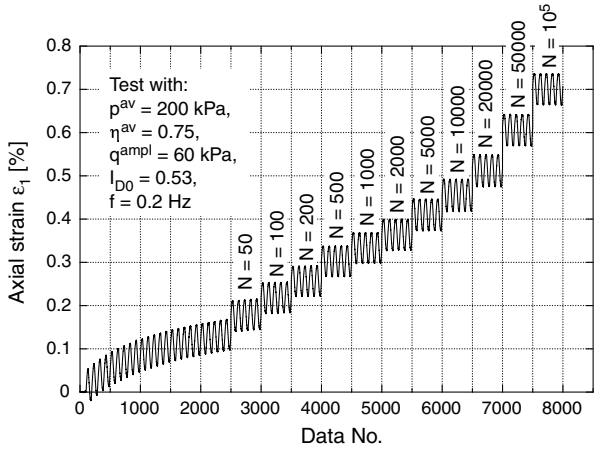

Figure 1. Vertical strain $\varepsilon_1(t)$ measured during the initial phase of a drained cyclic test and after different numbers of cycles.

The upper row of diagrams in Figure 2 shows the increase of the residual (= permanent, plastic) strain ε^{acc} with increasing number of cycles N measured in the four test series. Evidently, the rate of strain accumulation increases with increasing amplitude (Figure 2a), decreasing density (Figure 2c) and increasing average stress ratio (Figure 2g). Similar residual strains were obtained for different average mean pressures (Figure 2e) because the tests were performed with the same amplitude-pressure ratio $\zeta = q^{\text{ampl}}/p^{\text{av}}$ = 0.3.

The HCA model parameter C_{ampl} was determined from a curve-fitting of the function f_{ampl} (Table 1) to the data shown in Figure 2b. In that figure the residual strain ε^{acc} after different numbers of cycles is plotted versus a mean value of the strain amplitude, calculated as $\bar{\varepsilon}^{\text{ampl}} = 1/N \int \varepsilon^{\text{ampl}}(N)\mathrm{d}N$. This averaging is necessary since the tests have been performed stress-controlled and thus the strain amplitude decreases slightly with N (especially during the first 100 cycles). On the ordinate the residual strain has been divided by the void ratio function $\bar{f}_e$ of the HCA model in order to purify the data from the influence of slightly different initial densities and different compaction rates. $\bar{f}_e$ has been calculated with a mean value of void ratio $\bar{e} = 1/N \int e(N)\mathrm{d}N$. The parameter C_{ampl} given in Table 1 is the average of the values determined for different numbers of cycles.

A curve-fitting of the function f_e to the data in Figure 2d delivered the parameter C_e given in Table 1. In Figure 2d the residual strain has been divided by the amplitude function f_{ampl} in order to purify the data from the influence of slightly different strain amplitudes. The data are plotted versus a mean value of void ratio.

The parameters C_p and C_Y (Table 1) were determined from a curve-fitting of the functions f_p and f_Y to the data in Figures 2f and 2h. In those diagrams the residual strain has been divided by the amplitude and void ratio function and plotted versus p^{av} or $\bar{Y}^{\text{av}}$, respectively, where $\bar{Y}^{\text{av}}$ is a normalized stress ratio which is zero for isotropic stresses and 1 on the critical state line.

The curves $\varepsilon^{\text{acc}}(N)$ from Figure 2 have been divided by the functions $\bar{f}_{\text{ampl}}$, $\bar{f}_e$, f_p and f_Y of the HCA model (Figure 3) in order to determine the parameters C_{N1}, C_{N2} and C_{N3}. A curve-fitting of the function $f_N = C_{N1} \cdot [\ln(1 + C_{N2}\ N) + C_{N3}\ N]$ to the data in Figure 3 (solid curve) delivered the C_{Ni}-values specified in Table 1.

The critical friction angle $\varphi_c = 33.1°$ necessary for the cyclic flow rule **m** has been determined from the inclination of a pluviated cone of dry sand.

Isotropic elasticity is assumed for E in Eq. (1). Therefore, two elastic constants (e.g. bulk modulus K and Poisson's ratio ν) have to be determined. The bulk modulus $K = \dot{u}/\dot{\varepsilon}_v^{\text{acc}}$ can be obtained as the ratio of the rate of pore water pressure accumulation $\dot{u}$ in a stress-controlled undrained cyclic test and the rate of volumetric strain accumulation $\dot{\varepsilon}_v^{\text{acc}}$ measured in a drained test. Both samples should have similar initial densities and the tests should be performed with identical consolidation stresses and cyclic loads. Six such test pairs have been performed on the fine sand so far. All specimens were prepared medium dense and consolidated isotropically. Different initial effective mean pressures in the range 50 kPa $\leq p_0 \leq$ 300 kPa and different amplitude-pressure ratios in the range $0.2 \leq \zeta = q^{\text{ampl}}/p_0 \leq 0.3$ were tested (not all combinations have been tested so far). Based on the test results (documented in detail by Wichtmann et al. (2010)) the pressure-dependent bulk modulus can be described by

$$K \;=\; A\,(p_{\text{atm}})^{1-n}\,p^n \tag{3}$$

with p^{atm} = 100 kPa and with constants A = 467 and n = 0.46. No significant influence of the amplitude on K could be detected.

Poisson's ratio ν can be obtained from the shape of the average effective stress path in an undrained test with anisotropic consolidation stresses and strain cycles. A comprehensive test series on the fine sand is documented elsewhere (Wichtmann et al., 2010). A Poisson's ratio of $\nu \approx 0.32$ has been found appropriate for calculations with the HCA model.

The parameters of the hypoplastic constitutive model with intergranular strain are needed in the FE calculations for the determination of the spatial field of the strain amplitude. The parameters of the conventional hypoplastic model (Table 2) were determined according to Herle (1997). Drained monotonic triaxial tests on dense samples and oedometric compres-

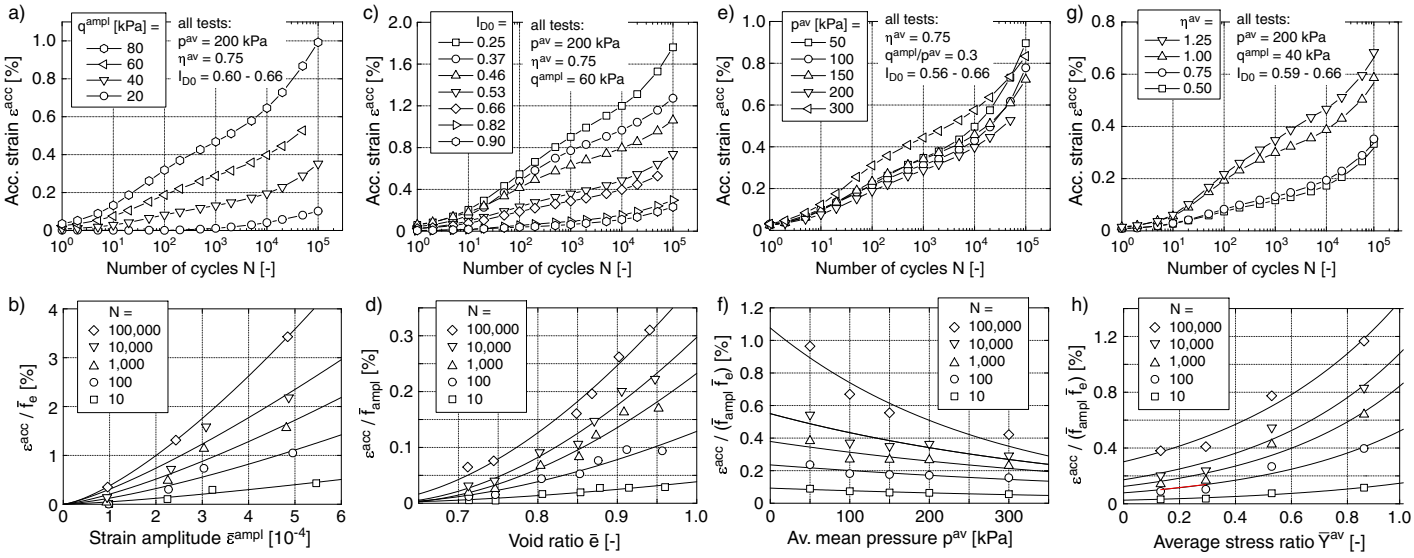

Figure 2. Results of drained cyclic tests with different a,b) amplitudes, c,d) initial relative densities I_{D0}, e,f) average mean pressures p^{av} and g,h) average stress ratios η^{av}.

Table 2. Hypoplastic parameters for the fine sand.

h_s	n	α	β	e_{i0}	e_{c0}	e_{d0}
[MPa]	[-]	[-]	[-]	[-]	[-]	[-]
862.6	0.32	0.21	1.5	1.212	1.054	0.677

Table 3. Parameters of intergranular strain for the fine sand.

R	m_T	m_R	β_R	χ
[-]	[-]	[-]	[-]	[-]
10^{-4}	2.3	4.6	0.2	2.8

sion tests on loose and dense samples were performed for that purpose.

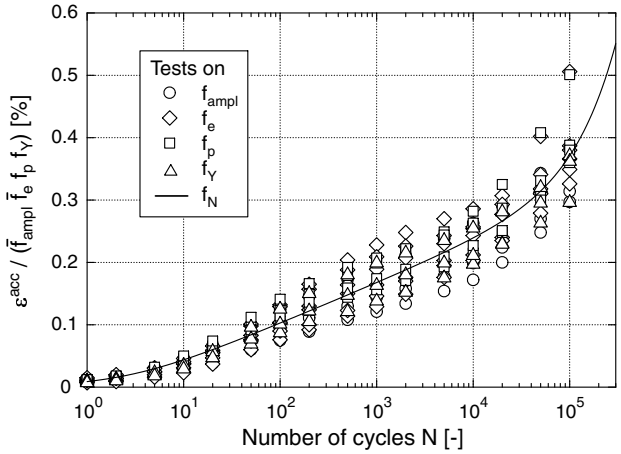

Figure 3. Determination of parameters C_{Ni} from a curve-fitting of the function f_N to the curves $\varepsilon^{\mathrm{acc}}(N)/(\bar{f}_{\mathrm{ampl}} f_e f_p f_Y)$.

The parameters of intergranular strain (Table 3) were chosen such way that the strain amplitude measured in a drained cyclic triaxial test with p^{av} = 200 kPa, η^{av} = 0.75 and q^{ampl} = 60 kPa is reproduced well.

5 FE CALCULATIONS

The FE calculations have been performed in order to prove the HCA model prediction qualitatively. The geometry of a real OWPP project (Figure 4) supplied by "Germanischer Lloyd Wind Energie GmbH" has been used. The inner and outer diameter of the monopile are d_i = 5.00 m and d_a = 5.09 m, respectively. The depth of embedding is 32.65 m. An erosion of the upper 3 m of the soil is likely to occur, thus only the lower 29.65 m were considered for the embedding.

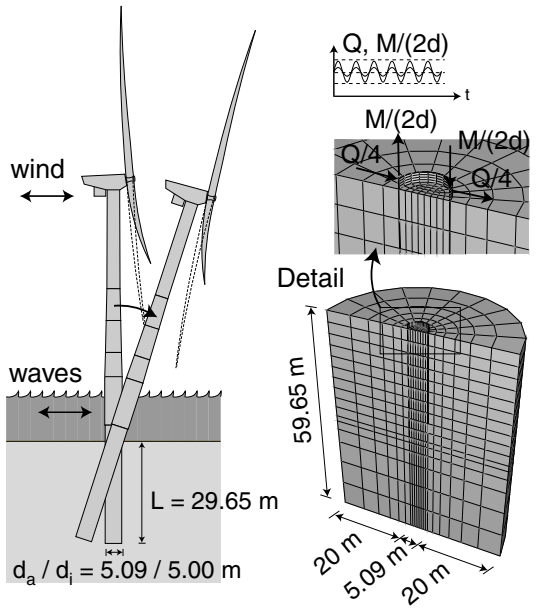

Figure 4. FE model of a OWPP monopile foundation.

The commercial program Abaqus 6.7 was used in combination with the user-subroutine Umat, in which both the hypoplastic model with intergranular strain and the HCA model are implemented. The 3D-FE dis-

cretisation is shown in Figure 4. Since only an unidirectional cyclic loading has been considered so far, the symmetry of the system could be utilized and only one half of the problem's geometry was modeled. Three-dimensional elements with reduced integration scheme (C3D8R) were used for the discretisation. Ten layers of elements were chosen along the depth of embedding and two elements were used for the thickness of the pipe. The soil was modeled within the radius of 20 m around the pile shaft and up to a depth of 20 m below the pile tip. The pile was modeled up to 1 m above the seabed. The Young's modulus of the steel pipe was $E = 2.1 \cdot 10^8$ kPa except the upper 1 m where it was chosen as $E = 10^{10}$ kPa in order to distribute the concentrated loads applied to the head of the pile. A Mohr-Coulomb contact with a friction coefficient μ = 0.3 was used at the inner and outer side of the steel pipe. The bending moment M was applied as a pair of vertical forces acting on two nodes laying on the symmetry axis (Figure 4). The shear force Q was also equally distributed to these two nodes. The vertical load V due to the own weight of the OWPP tower was distributed equally to all nodes at the top of the pile. A uniform distribution of the initial void ratio was assumed. The initial earth pressure coefficient at rest was set to K_0 = 0.5.

The loading was applied in the following steps:

1. Application of the self weight of the soil with the geostatic initial stress (without generating deformations).
2. Application of the vertical force V = 9247 kN representing the own weight of the tower.
3. Application of the average values of the bending moment (M^{av}) and the shear force (Q^{av}).
4. Calculation of the first cycle, using the hypoplastic model with intergranular strain. The loading was applied sinusoidal with the amplitudes M^{ampl} and Q^{ampl}.
5. Calculation of the second cycle, using the hypoplastic model with intergranular strain. During the cycle, the strain path was recorded in each integration point. The spatial field of the strain amplitude was determined from that strain path and is input for the following calculation with the HCA model.
6. Calculation of permanent deformations due to $N = 10^6$ cycles using the HCA model. The bending moment and the shear force were kept constant at their average values M^{av} and Q^{av} while the permanent deformations due to the cyclic loading with M^{ampl} and Q^{ampl} were predicted by the HCA model.

Calculations with different amplitudes M^{av} and average values M^{ampl} of the bending moment were performed. The chosen values cover the design range for real OWPP projects. A constant ratio Q/M = 0.027 1/m of shear force and bending moment was set into approach. Figure 5a presents the lateral pile displacements after $N = 10^6$ cycles applied with different amplitudes in the range 10 MNm $\leq M^{\text{ampl}} \leq$ 25 MNm. Results from calculations with different average values 20 MNm $\leq M^{\text{av}} \leq$ 50 MNm of the bending moment are shown in Figure 5b, while Figure 5c provides the lateral displacement for different initial relative densities in the range $0.5 \leq I_{D0} \leq 0.9$. The predicted increase of the permanent lateral displacements with increasing amplitude M^{ampl}, increasing average value M^{av} and decreasing initial density could be expected from the cyclic triaxial test results (Figure 2b) and is in accordance with model test data (Hettler, 1981; Long and Vanneste, 1994; Lin and Liao, 1999).

A quantitative verification of the HCA model prediction based on model tests performed on the fine sand and (if available) in situ data is planned for the future. For a shallow foundation the HCA model prediction has been already proven by recalculations of a centrifuge model test (Niemunis et al., 2005).

6 SUMMARY, CONCLUSIONS AND OUTLOOK

The paper discusses a possible application of the authors' high-cycle accumulation (HCA) model for the prediction of permanent deformations of OWPP foundations. The calibration of the HCA model for a typical North Sea fine sand is presented. The parameters have been used for finite element calculations of a real OWPP project founded on a monopile. The predicted increase of the permanent lateral displacements with increasing amplitude and average value of the applied bending moment and with decreasing soil density is qualitatively plausible and in accordance with model test results in the literature. A quantitative verification of the HCA model prediction is planned for the near future.

Several series of cyclic triaxial tests will be performed on the fine sand in order to further develop the HCA model, in particular with regard to the application to OWPP foundations. Since the OWPP foundations are subjected to a very large number of load cycles, long-term tests with $N \approx 10^8$ cycles are planned in order to evaluate the function f_N of the HCA model for large N-values. The effect of changes of the polarization of the cycles (factor f_π of the HCA model) will be studied in cyclic triaxial tests with a simultaneous oscillation of the axial and lateral stresses. In the case of OWPPs such changes are caused by the variation of the direction of wind and wave loading.

7 ACKNOWLEDGEMENTS

This work has been done in the framework of the project "Geotechnical robustness and self-healing of foundations of offshore wind power plants" funded

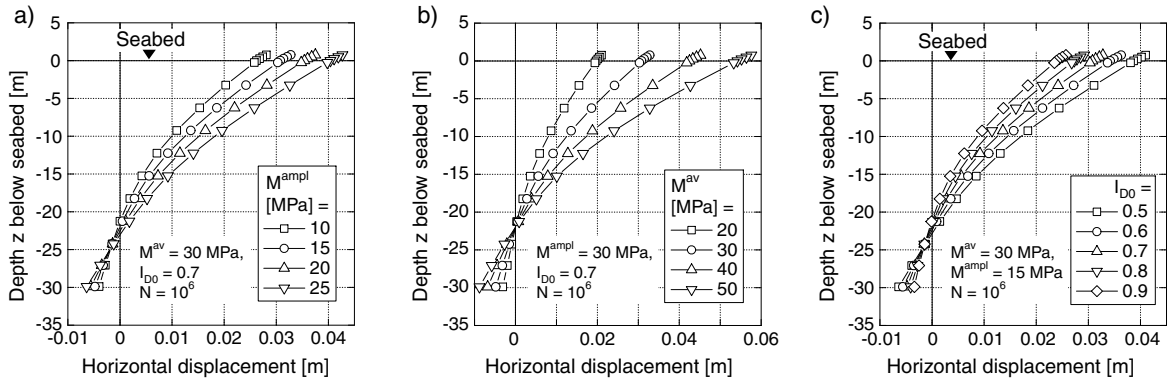

Figure 5. Results of FE calculations: Horizontal displacement of the monopile as a function of depth z below seabed, calculated for different amplitudes and average values of the bending moment.

by the German Federal Ministry for the Environment, Nature Conservation and Nuclear Savety (BMU) (grant No. 0327618). The authors are grateful to BMU for the financial support. Furthermore, the authors wish to thank H. Borowski who performed the cyclic triaxial tests.

REFERENCES

Achmus, M., Abdel-Rahman, K. & Kuo, Y.-S. 2008. Design of monopile foundations for offshore wind energy converters. In Z. Mlynarek, Z. Zikora, and E. Dembicki, editors, *Goetechnics in Maritime Engineering, Proc. of 11th Baltic Sea Geotechnical Conference*, 1:463-470.

American Petroleum Institute (API). 1993. Recommended Practice for Planning, Designing and Constructing Fixed Offshore Platforms - Working Stress Design. API RP 2A - WSD, Vol. 20, Dallas.

Dührkop, J. 2010. Zum Einfluss von Aufweitungen und zyklischen Lasten auf das Verformungsverhalten lateral beanspruchter Pfähle in Sand. Dissertation, Veröffentlichungen des Institutes für Geotechnik und Baubetrieb der Technischen Universität Hamburg-Harburg, Heft Nr. 20.

Germanischer Lloyd. 2005. Rules and Guidelines, IV Industrial Services, 2 Guideline for the Certification of Offshore Wind Turbines, 6 Structures.

Herle, I. 1997. Hypoplastizität und Granulometrie einfacher Korngerüste. Promotion, Institut für Bodenmechanik und Felsmechanik der Universität Fridericiana in Karlsruhe, Heft Nr. 142.

Hettler. A. 1981. Verschiebungen starrer und elastischer Gründungskörper in Sand bei monotoner und zyklischer Belastung. Institut für Boden- und Felsmechanik der Universität Karlsruhe, Heft Nr. 90.

Lesny K. & Hinz, P. 2006. A concept for a safe and economic design of foundations for offshore wind energy converters. In *New Approach to Harbour, Coastal Risk Management and Education, Proc. of LITTORAL 2006, Gdansk, Poland*, 90-98.

Lin, S.-S. & Liao, J.-C. 1999. Permanent Strains of Piles in Sand due to Cyclic Lateral Loads. *Journal of Geotechnical and Geoenvironmental Engineering, ASCE*, 125(9):798-802.

Little, R.L. & Briaud, J.-L. 1988. A pressuremeter method for single piles subjected to cyclic lateral loads in sand. Technical Report GL-88-14, US Army Corps of Engineers.

Long, J.H. & Vanneste, G. 1994. Effects of cyclic lateral loads on piles in sand. *Journal of Geotechnical Engineering, ASCE*, 120(1):225-244.

Niemunis, A. & Herle, I. 1997. Hypoplastic model for cohesionless soils with elastic strain range. *Mechanics of Cohesive-Frictional Materials*, 2:279-299.

Niemunis, A., Wichtmann, T. & Triantafyllidis, T. 2005. A high-cycle accumulation model for sand. *Computers and Geotechnics*, 32(4):245-263.

Reese, L.C., Cox, W.R. & Koop, F.D. 1974. Analysis of laterally loaded piles in sand. In *Proceedings of the 6th Annual Offshore Technology Conference, Houston, Texas, OTC 2080*, pages 473-458.

Swinianski, J. & Sawicki, A. 1991. A model of soil pile interaction owing to cyclic loading. *Canadian Geotechnical Journal*, 28(1):11-19.

Det Norske Veritas. 2004. Offshore Standard DNV-OS-J101: Design of Offshore Wind Turbine Structures.

von Wolffersdorff, P.-A. 1996. A hypoplastic relation for granular materials with a predefined limit state surface. *Mechanics of Cohesive-Frictional Materials*, 1:251-271.

Welch R.C. & Reese, L.C. 1972. Laterally loaded behavior of drilled shafts. Technical Report 3-5-65-89, Center for Highway Research, University of Texas, Austin.

Wichtmann, T., Rojas, B., Niemunis, A. & Triantafyllidis, T. 2010. Stress- and strain-controlled undrained cyclic triaxial tests on a fine sand for a high-cycle accumulation model. In *Proc. of the Fifth International Conference on Recent Advances in Geotechnical Earthquake Engineering and Soil Dynamics, San Diego, USA*.